**AFRC Industrial Combustion Symposium**
**September 10-12, 2022**
**Greenville, SC**

# A Bayesian Decision-Theory-Based Digital Twin for Methane Flares

Jebin Elias (jebin.elias@utah.edu)
Jennifer P. Spinti (jennifer.spinti@utah.edu)
Sean T. Smith (sean.t.smith@utah.edu)
Philip J. Smith (philip.smith@utah.edu)
**The University of Utah, Salt Lake City, UT 84112**

Jeremy Thornock (jthornock@gmail.com)
**Lawrence Livermore National Laboratory, Livermore, CA 94550**

Marc Cremer (cremer@reaction-eng.com)
Minmin Zhou (zhou@reaction-eng.com)
**Reaction Engineering International, Salt Lake City, UT 84047**

# 1 Abstract

Ground flares operate in a high-turndown, standby configuration for a significant portion of their operating life, being fully utilized only under process upset scenarios or emergencies. The low-momentum flow results in poor fuel-air mixing near the flare tip, leading to decreased overall combustion efficiency (CE) and increased emissions of unburnt volatile organic compounds (VOC). In such scenarios, assist medium flow rates that are too low, a state called under-assist, results in excessive visible smoke and particulate pollution. On the other hand, over-assisting degrades CE due to premature quenching of the reaction zones. Prevailing wind conditions directly impact the CE of a flare by promoting mixing to varying degrees. Fluctuating wind gusts also generate turbulence near the flare tip, occasionally inducing fuel stripping from the reaction zones, or creating intermittent puffs of flame due to localized change in the equivalence ratio. Therefore, achieving continuous smokeless flaring while maintaining high overall combustion efficiency ($CE_{overall}$) requires active control of the fuel and assist streams based on the local environmental conditions.

It is, however, difficult to measure the $CE_{overall}$ of an open flare in crosswind and even more challenging to quantify the uncertainty in that measurement. An approximation to this quantity of interest (QOI) may be made with a remote sensing device such as a Passive Fourier Transform Infrared Spectrometer (PFTIR). In the previous work[1], we demonstrated the power of the application of Bayes' law using both simulation and experimental PFTIR data in determining the uncertainty in the PFTIR measurements of the CE ($CE_{PFTIR}$) for a range of net heating values of the combustion zone ($NHV_{cz}$). With this approach, we simultaneously validated the test data collected at the John Zink Flare Facility using a John Zink steam-assisted SKEC flare at high turndown[2] with the simulation data of the same flaring configurations using the multi-physics Uintah-Arches simulation tool. In this *machine-learning stage* of the digital twin, we also computed $CE_{overall}$ and its uncertainty in the absence of any measured data as a Bayesian posterior predictive.

In the current *decision-making stage*, the Bayesian decision-theory-based digital twin actively operates on the local wind information and quantifies the trade-offs among decisions on steam-assist mass flow rate based on the utility and economics of the flare operation. The digital twin evaluates all possible decisions from the joint posterior distribution of the uncertain system parameters derived at the *machine-learning stage*[1] to maximize the expected utility. It then prescribes an operational set point for the steam-assist mass flow rate and predicts the $CE_{overall}$ with specified uncertainty at the optimized set point. This feedback circuit serves to monitor and control the flare operation actively. The results demonstrate that the active control of the flare based on the digital twin response allows the flare to be operated at significantly higher $NHV_{cz}$ while improving the $CE_{overall}$ over a range of operating conditions. Optimizing the steam-assist mass flow rates based on the local wind conditions also yields predictions of $CE_{overall}$ with a lower uncertainty margin than when not correcting the assist stream mass flow rate for crosswind effects.

## 2 Introduction

John Vickers, a principal technologist at NASA, first proposed the concept of 'digital twins' for engineering scenarios[3] during the Apollo Space Program of NASA. Michael Graeves[4] further propagated the concept as a product life cycle management tool, "a re-engineering of structural life prediction and management." The concept evolved over the years[5,6], taking many different forms based on the domain of application. It has been gaining popularity, especially in data-driven design processes, manufacturing, automation, space exploration, hydrocarbon exploration, etc. In engineering, digital twins are virtual copies of the asset that operate on the same input parameter space and produce the same output streams and more. The digital twin is critical to effective decision-making in industries and can be used in automated systems that actively monitor a plant operation. A digital twin is, therefore, an adaptive and comprehensive virtual replica of a physical system that can mirror the system across its entire operating range/life cycle and evolve with it[7].

Versions of the digital twin have been successfully applied to combustion systems (mainly furnaces and boilers) in recent years[8–10]. These digital twins control the system based on pre-defined rules, eliminating human involvement. The mapping of an operating condition to a decision is however, not performed actively, rendering the digital twin unable to learn from and adapt with the system. An advanced, data-driven, neural network-based set-point determination for flares, demonstrated by Damodara et.al.[11], actively learns from the data to adjust its response characteristics. While this model continuously evaluates new data to update the decisions, it fails to predict operational set-points outside the range of the specified test conditions owing to the complex nature of the interaction of an open industrial flare and its surroundings due to fluctuating wind conditions and to the inherent difficulty in quantifying $CE_{overall}$ using remote sensing techniques alone. Spinti et.al.[12] applied Bayesian inference to quantify the uncertainties in multiple parameters that define the performance characteristics of a biomass boiler power plant. Propagating the uncertainties forward, they computed posterior predictives of multiple QOIs, which will feed a decision-making model that determines the optimal set-point for the operating variable of the boiler in the presence of uncertainty.

In contrast to other data-driven methods, a Bayesian digital twin contains full knowledge of its historical performance in the form of priors ($p(\mathbf{X})$, and has the ability to learn from the data and to change in conformity with the real system by re-evaluating the inverse problem ($p(\mathbf{X}|\mathbf{Y})$) when newer data is presented. The *decision-making* part solves the forward problem of Bayes' Law ($p(\mathbf{Y}|\mathbf{X})$) to predict $CE_{overall}$ from the posterior distribution and employs a cost-utility function to facilitate decision-making. The decision, a set-point for the steam-assist mass flow rate, is obtained by maximizing the expected utility. As with the previous stage, the *decision-making stage* uses data from multiple experiments on the John Zink steam-assisted ground flare in crosswind[2] along with LES results from a suite of multi-scale simulations performed using the Uintah-Arches multi-physics simulation package.

## 3 Bayesian Decision Theory

Bayesian-inference-based decision theory models are statistical models that provide guidelines for making decisions in the presence of known uncertainties and that classify decisions by quantifying the trade-offs among them using probabilities and cost evaluations. This type of decision-theory model is best used in live engineering systems with active feedback. With the feedback acting as the input, the model can update the controller set-points based on the new, uncertain information and the knowledge of the historical behavior of the system. It is, therefore, a simplistic way of performing artificial intelligence for the engineering problem at hand[13].

Every decision has a utility and cost associated with it. Normative decision theory models are grounded on mathematical relationships between the decisions and the associated utility and cost. With expected value theory, a subset of normative decision theory, every decision is weighted according to its utility and cost by assigning probabilities to each decision.

A *decision* in a Bayesian context is a combination of values from the posterior distribution of the uncertain parameters. Denoting the decision space (collection of all possible decisions) as $\mathbf{X}_d$ and an individual decision as $x_d$ such that $x_d \in \mathbf{X}_d$, the probability of the outcome of a decision can then be represented by $p(y_d|x_d)$, and the collection of all possible outcome can be denoted by $\mathbf{Y}_d$ such that $y_d \in \mathbf{Y}_d$.

Decision-making also involves assigning a subjective cost to each decision that reflects the preference for obtaining that outcome. Decisions involving multiple parametric dimensions may include multiple cost models with different weightage that sum to the overall cost. A utility function, defined based on the outcome of the decision written as $\mathscr{U}(y_d)$, quantifies the value of a decision $x_d$ based on its cost and the risk involved in the decision. Expected value based decision-making use of these explicit utility value assigned to different outcomes combined with the probability of those outcomes to guide the choice between options.

According to the normative decision theory, the best decisions maximize the expected value ($\mathscr{E}()$) of the utility function, which is the sum of the utility of every possible outcome, each multiplied by the probability of its occurrence. Mathematically, it can be written as :

$$\max\left( \mathscr{E}\left(\mathscr{U}(y_d)\right) \right) = \max\left( \int \mathscr{U}(y_d)\, p(y_d|x_d)\, \mathrm{d}y_d \right) \tag{1}$$

For the SKEC flare, a decision is an optimised steam-assist mass flow rate for a specific wind speed that promotes smokeless flaring with the highest achievable operational $CE_{overall}$.

# 4 Decision Space and Decision-Making

A decision space for a digital twin may be defined as the parametric space within which all decisions lie. The simplest decision spaces are bounded by the limits of the various uncertain parameters of the system and the range of QOIs. An alternate approach to defining the decision space is by solving the Bayesian inverse problem involving these uncertain parameters, yielding a posterior distribution that better represents the collection of decisions that is consistent with all of the measured data.

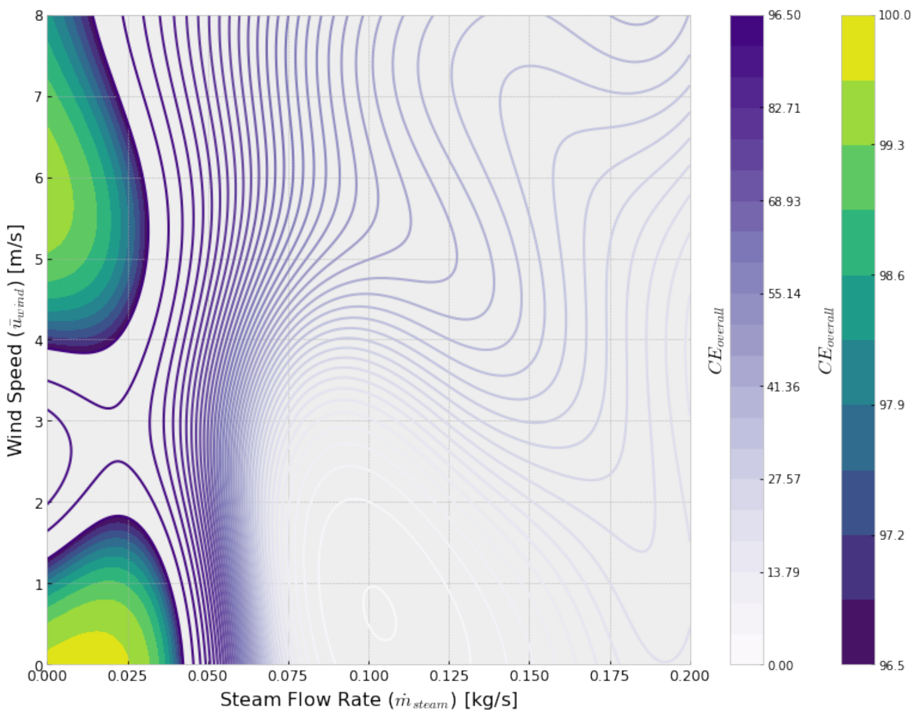


**Fig. 1.** Decision space of the SKEC flare digital twin. Every point in the contour, defined by a wind speed and steam-assist mass flow rate, has a distribution of $CE_{overall}$. The image is a slice of the mode of these distributions at all possible pairs. The filled contour is truncated below 96.5% of $CE_{overall}$ to highlight the targeted optimal performance region. Contour lines below 96.5% show the gradient in the $CE_{overall}$ prediction for the full parametric space.

For the SKEC steam-assisted flare, the decision space is three-dimensional with ambient wind speed as an input and the steam-assist mass flow rate and $CE_{overall}$ as the parameters of a decision model. Figure 1 shows the slice at the mode of the predicted distribution of $CE_{overall}$ for every possible pair of wind speed and steam-assist mass flow rate. In the absence of reliable methods to measure $CE_{overall}$ in-situ, EPA regulations based on studies conducted on open industrial flares[14], prescribe the flare to be operated above $NHV_{cz}$ of 270 $BTU/scf$ to maintain an operational CE of $98 \pm 1.5\%$ at all times. This targeted performance band is highlighted in

Figure 1. Given the local wind condition (any point in the y-axis of Figure 1), the primary consideration for any flaring operation is to achieve high $CE_{overall}$ with a stable flame that promotes smokeless flaring[15,16].

For low wind speeds at low steam-assist mass flow rates, the turbulent mixing near the flare tip improves air entrainment into the plume, which promotes complete combustion (high $CE_{overall}$). Over-assist in such a scenario degrades the $CE_{overall}$, as seen by the steep gradients in the profile (refer to Figure 1). The cooling effect from over-assist may also inhibit dispersion of flared gases. At higher wind speeds, the steam-assist mass flow rate has a lesser impact on $CE_{overall}$. However, depending on the local conditions, the flame may destabilize and enter a smoking phase due to poor local mixing resulting in insufficient oxidizer in the reaction zone. This degrades $CE_{overall}$, increases the VOC emissions, and generates smoke. In extreme cases, over-steaming at high wind speed can snuff out a flame and allow waste gases to escape unburned. There is hence an optimal steam-assist mass flow rate for every wind condition that yields the best combustion characteristics for the flare.

### 4.1 Decision Model

Multiple regulatory conditions are imposed on flare operations to limit the environmental impact while ensuring the highest performance. In a decision-making context, such conditions are called decision constraints, as they collectively define rules for comparing acceptable values for the decision variables. By representing these conditions as mathematical relations, we assign numerical values to the parameters of the decision space and the corresponding outcome. These mathematical expressions are called cost models for the parameters. An 'integrated' cost model applicable across the entire decision space is assembled by combining the cost models.

The main considerations for the decision-making for SKEC flares are:

- EPA regulations prescribe flare operational CE to be within $98 \pm 1.5\%$ at all times except for a period of five minutes over any two hour time window[14,16].
- In the absence of methods to accurately measure $CE_{overall}$ of the flare, maintaining the flare $NHV_{cz}$ above 270 $BTU/scf$ is assumed to ensure a $CE_{overall}$ of $98 \pm 1.5\%$[14,16]. For the SKEC tests, this translates into 0.022 $kg/s$ of steam when the fuel flow rate is maintained at $4 ft/s$.
- Avoid excessive smoking. There is a higher probability for the flame to start smoking in pockets within the high temperature reaction zone with a higher equivalence ratio.

Figure 1 highlights the region with the best performance for every wind condition. For steam flow rates $\leq 0.022 kg/s$, there is a higher probability of achieving high $CE_{overall}$ for low and high wind speeds than for intermediate wind speeds. Bayesian decision theory is relevant in such scenarios where the optimization of the steam-assist mass flow rate considering the uncertainty in the measurement of wind speed and $CE_{overall}$ directly impacts the overall performance of the flare.

The constraints on the operation of the flare are formalized into a decision model as individual cost functions.

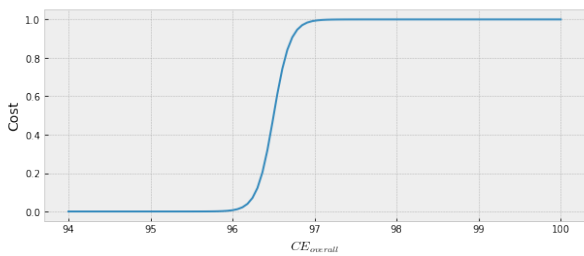


**Fig. 2.** Cost function for $CE_{overall}$.

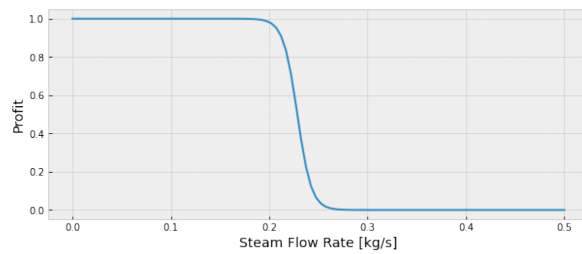


**Fig. 3.** Cost profile for steam-assist mass flow rate.

- **Constraint on Combustion Efficiency ($CE_{overall}$):** As per the EPA guidelines, the flares are to be operated at $CE_{overall} = 98 \pm 1.5\%$. This constraint can be expressed as a smooth step function (refer to Figure 2):

$$C_{CE} = 1 - \frac{1}{1 + exp\left[10 \cdot (y_{CE} - 96.5)\right]} \tag{2}$$

  The cost function assigns a higher value to decisions that yield $CE_{overall}$ higher that 96.5%.

- **Constraint on Net Heating Value of Combustion Zone ($NHV_{cz}$):** As per studies conducted by EPA [14], it is mandated that the flare $NHV_{cz}$ is maintained above 270 $BTU/scf$ to maintain the flare at $CE_{overall} = 98 \pm 1.5\%$ . Translating this into steam-assist mass flow rate condition, the constraint (refer to Figure 3) can be expressed as:

$$C_{\dot{m}_{steam}} = \frac{a}{20 \cdot (\frac{1}{2} + exp\left[50 \cdot (y_{CH_4} - 0.22)\right]} \tag{3}$$

  This cost function prefers the decisions where steam-assist mass flow rates are $\leq$ 0.022 $kg/s$ over the higher assist rates.

The composite cost function is written as:

$$C = w_1 \cdot C_{CE} + w_2 \cdot C_{\dot{m}_{steam}} \tag{4}$$

where $w_1$ and $w_2$ are the weights signifying the contribution of each individual cost function to the overall decision model. Adjusting these weights adjusts the sensitivity of the decision to each of the constraints.

The constraints described above are mere examples inferred/derived from the sparse data available for the SKEC flare. With better monitoring of other auxiliary parameters (fuel composition, fuel flow rate, steam pressure and temperature, humidity, etc.) additional constraining functions can be implemented within the decision model to better define the cost relationship.

### 4.2 Utility of a Decision

More often than not, the cost of a decision is not directly proportional to the utility of the said decision. An optimal decision is the one that considers all the risks involved to guide the decision-making. We employ an iso-elastic utility function to represent the level of desirability of each outcome in the presence of risk. The mathematical form is as below:

$$U(y_d) = \begin{cases} \frac{y_d^{1-\eta}-1}{1-\eta}, & \text{if } \eta \geq 0, \eta \neq 1 \\ \\ ln(y_d), & \text{if } \eta = 1 \end{cases} \tag{5}$$

where $\eta$ defines the degree of risk aversion. A low value of $\eta$ (*risk averse* mode) yields a more predictable but possibly lower payoff decision while a higher value of $\eta$ (*risk seeking* mode) yields a potentially higher payoff but possibly higher uncertainty.

### 4.3 Maximising the Expected Utility

The expected utility of a decision is the average utility value of all possible decisions weighted by the probability of that decision. Mathematically, the expected utility of a decision ($y_d$) is defined as:

$$\mathscr{E}\left(\mathscr{U}(y_d)\right) = \int \mathscr{U}(y_d)\, p(y_d|x_d)\, \mathrm{d}y_d \tag{6}$$

where $x_d$ is a decision, $y_d$ is the cost of that decision, $U(y_d)$ is the utility of that decision, and $p(y_d|x_d)$ is the probability of that decision occurring. By using Bayesian statistics and probability in combination with an optimizer, we make a decision that maximizes expected utility in the presence of uncertainty.

## 5 Posterior Predictions Based on Decision Theory

Evaluating the expected utility based on the cost of all possible decisions for a specific wind speed yields an optimised steam-assist mass flow rate (operational set-point) that satisfies all constraints of the decision model in the best possible manner.

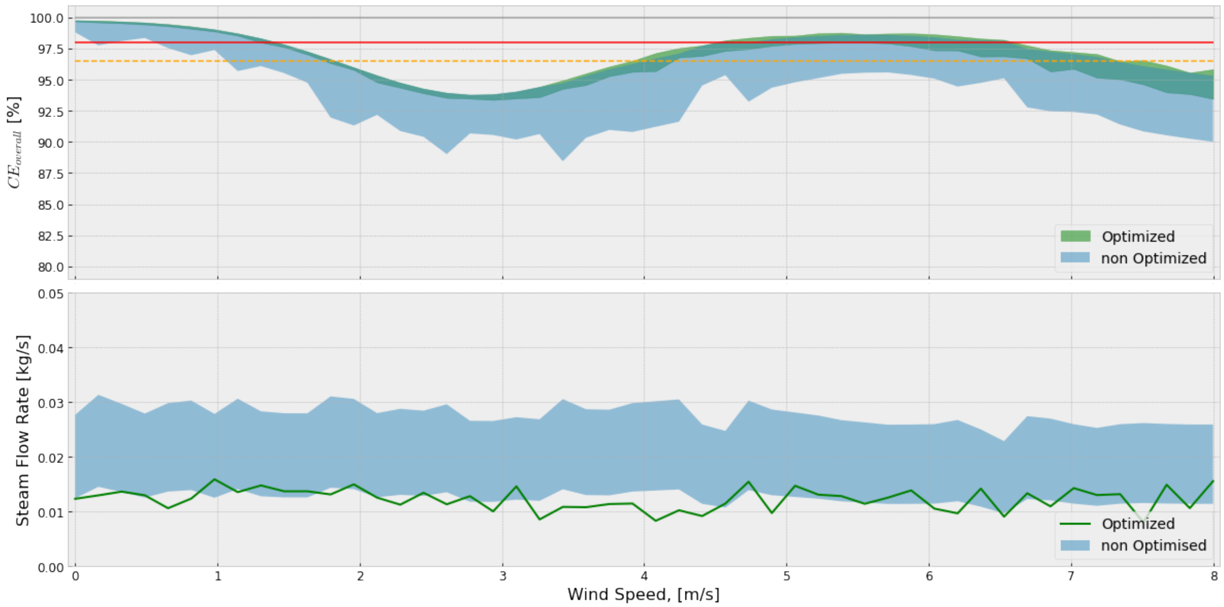


**Fig. 4.** (Top) Prediction of $CE_{overall}$ with optimized steam-assist mass flow rate (green) vs. the predictions of $CE_{overall}$ when steam-assist mass flow rate has the measurement uncertainty (blue). EPA mandated limit is shown as a red line at 98% and the allowable variability is represented by the orange line at 96.5%. (Bottom) Optimised steam-assist mass flow rate for every wind condition vs. as-measured steam-assist mass flow rates with quantified uncertainty.

## Overall Combustion Efficiency

The top half of Figure 4 shows the distribution of $CE_{overall}$ predictions when the flare is operated with the optimized steam-assist mass flow rate based on the local wind (green fill). In comparison, the blue fill shows $CE_{overall}$ predictions without optimisation that include the uncertainty in the steam-assist mass flow rate measurements; these predictions have a larger uncertainty than the optimized set-point for every wind condition. The bottom half of Figure 4 shows the optimized steam-assist mass flow rate and the steam-assist mass flow rate measurements with uncertainty for all possible wind conditions. These results show that the flare can be operated at steam flow rates below $0.022 kg/s$ (corresponding $NHV_{cz} \geq 270$ $BTU/scf$) while maintaining a high operational $CE_{overall}$ for almost all wind conditions. The predictions for $CE_{overall}$ closely match the expectation from the decision space mapping (Figure 1) for the optimized steam-assist mass flow rate, where there is a lower probability of finding steam-assist mass flow rates that ensure meeting the standards on the flare efficiency, for moderate wind speeds. While the optimization fails to determine a steam-assist mass flow rate for moderate wind conditions that results in the operational $CE_{overall}$ being above the prescribed limits, the digital twin successfully predicts the steam-assist mass flow rate that yields the best outcome from the decision model with quantified uncertainty.

### Degree of Risk Aversion

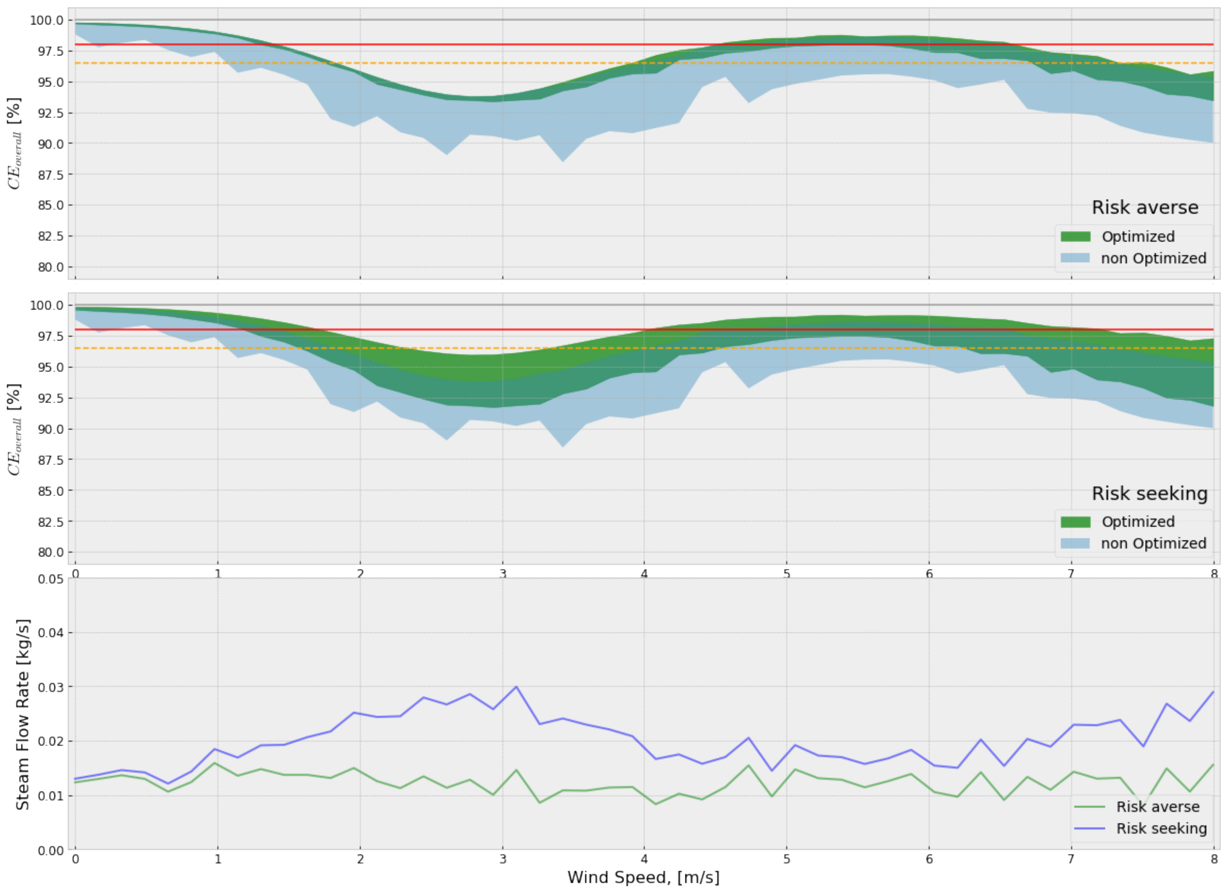


**Fig. 5.** Prediction of $CE_{overall}$ when the decision is made in (top) a risk-averse context and (middle) a risk-seeking context. The bottom plot shows the optimized steam-assist mass flow rate in both scenarios.

In Figure 5, we evaluate risk aversion in the decision-making process. This figure compares the distribution of $CE_{overall}$ given (top) risk-averse ($\eta = 1.0$) decision-making and (middle) risk-seeking ($\eta = 10.0$) decision-making. The risk-averse utility function guides the decision-making to target decisions with lower uncertainty even though $CE_{overall}$ is low while the risk-seeking utility function makes decisions that yield higher values for $CE_{overall}$ while accepting larger uncertainties in those outcomes.

For all wind speeds, a risk-averse strategy results in narrow distributions for the $CE_{overall}$ predictions that gradually widen with increasing wind speeds. With a risk-seeking strategy, the distributions of the $CE_{overall}$ predictions are wider at moderate and high wind speeds where the optimizer accepts steam-assist mass flow rates higher than 0.022 kg/s and higher uncertainties in the $CE_{overall}$ to attain higher probability of maintaining a higher $CE_{overall}$.

## Dynamic Application of Digital Twin

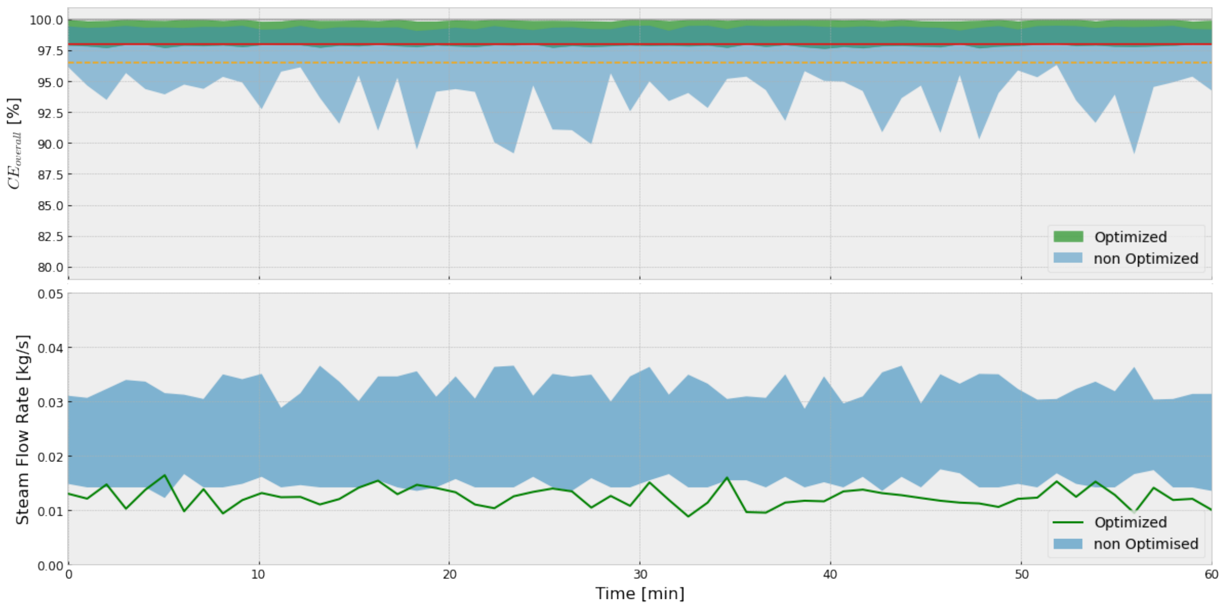


**Fig. 6.** (Top) Dynamic digital twin predictions of $CE_{overall}$. at the optimized steam assist flow rate compared against the $CE_{overall}$ predictions based on the uncertainties in the scenario parameters (wind speed and steam-assist mass flow rate). (Bottom) Optimised mass flow rate of steam compared against the distribution of steam-assist mass flow rate when no optimization is applied.

While instantaneous $CE_{overall}$ predictions of the flare performance are helpful in understanding the combustion characteristics and operation of the flare, a comprehensive assessment of the flare performance over a period of time is essential in quantifying the amount of VOC emissions from the flare and in evaluating whether the flare meets other environmental and regulatory constraints. Figure 6 shows the flare performance within a one hour time window assuming that the flare operates with the optimized steam flow rate updated every minute of flare operation. Matching the wind characteristics to the test data for the duration of this time window, $CE_{overall}$ predictions with the optimised steam assist set-point are consistently above the regulatory constraint of 98% (green fill); the time-averaged value of $CE_{overall}$ is 97.89%. The optimized steam-assist mass flow rate is also low, ensuring that the flare operates above a $NHV_{cz}$ of 270 $BTU/scf$. Without the optimization for steam-assist mass flow rate, the $CE_{overall}$ predictions have large uncertainties that extend well below the target limits; the time-averaged value of $CE_{overall}$ is 90.69%. A higher average $CE_{overall}$ implies significant reductions in total VOC emissions over time and cleaner flaring.

# 6 Conclusions

Open industrial flares under crosswind are subject to strict regulations on operating conditions to achieve acceptable levels of $CE_{overall}$, emissions, and visible smoke. With several factors affecting each of these performance metrics, combined with the uncertainty in measuring the post-combustion plume to verify the operational characteristics of the flare, we have developed a digital twin in order to model, learn from, and actively control the system.

In the *machine-learning stage*[1] of the digital twin, we determined the uncertainty in the measured quantities of a SKEC flare at high turndown, which helped define an operating envelope for the flare, and predict with confidence, quantities that could not be measured accurately. In the *decision-making stage* described in this paper, we defined a three-dimensional decision space around the operating envelope that collects all possible decisions and their outcomes. We then created cost functions to represent the flare operational constraints and applied an iso-elastic utility function to the output of the cost (decision) model. By maximizing the expected utility among decisions for any wind speed specification, we compute an optimized steam-assist mass flow rate that best satisfies the decision constraints.

With this digital twin, we computed posterior predictive values of $CE_{overall}$ at the optimized steam-assist mass flow rate for different operating conditions (i.e., wind speeds). These values show significant improvement in comparison with the predictions of $CE_{overall}$ using the non-optimized steam-assist mass flow rates and accounting for their uncertainty.

This paper demonstrates the capability of a Bayesian decision-theory-based digital twin in predicting the performance of a flare operating at high turndown. With an on-site anemometer actively reporting ambient wind conditions, the digital twin can be implemented in an automated control system to monitor and control the flare and can generate operational summary reports for a prescribed period of time that evaluate the long-term operational cost, total VOC emissions, and other flare data both measured and unmeasured. This methodology could be applied to other flares in other operating regimes following the principles outlined here.

## Acknowledgments/Disclaimer

This material is based upon work supported by the U.S. Department of Energy, Office of Science, under Award Number DE-SC0017039. The authors wish to thank Dan Pearson and Scott Evans at Clean Air Engineering for answering our many questions related to the flare test data. This paper was prepared as an account of work sponsored by an agency of the United States Government. Neither the United States Government nor any agency thereof, nor any of their employees, makes any warranty, express or implied, or assumes any legal liability or responsibility for the accuracy, completeness, or usefulness of any information, apparatus, product, or process disclosed, or represents that its use would not infringe privately owned

rights. Reference herein to any specific commercial product, process, or service by trade name, trademark, manufacturer, or otherwise does not necessarily constitute or imply its endorsement, recommendation, or favoring by the United States Government or any agency thereof. The views and opinions of authors expressed herein do not necessarily state or reflect those of the United States Government or any agency thereof.

## References


[1] Jebin Elias, Jennifer C. Spinti, Sean T. Smith, Philip J. Smith, Jeremy N. Thornock, Marc Cremer, and Minmin Zhou. A Bayesian Approach to Quantifying the Uncertainty of Combustion Efficiency Measurements in Flares. In *American Flame Research Committee 2021 Industrial Combustion Symposium*, October 2021.

[2] Clean Air Engineering Inc. Performance Test of Steam-Assisted and Pressure Assisted Ground Flare Burners with Passive FTIR – Garyville. Technical report, Marathon Petroleum Company, LP, 2013. Project No: 12082.

[3] Bob Piascik, John Vickers, Dave Lowry, Steve Scotti, Jeff Stewart, and Anthony Calomino. Materials, Structures, Mechanical Systems, and Manufacturing Roadmap. *NASA TA*, pages 12–2, 2012.

[4] Michael Grieves. *Origins of the Digital Twin Concept*, 08 2016.

[5] M. Grieves. *Product Lifecycle Management: Driving the Next Generation of Lean Thinking: Driving the Next Generation of Lean Thinking*. McGraw-Hill Education, 2005. ISBN 9780071786300. URL https://books.google.com/books?id=rYwkg-C-pm0C.

[6] Michael Grieves. *Virtually perfect: driving innovative and lean products through product lifecycle management*. Space Coast Press, 2011.

[7] D. J. Wagg, K. Worden, R. J. Barthorpe, and P. Gardner. Digital Twins: State-of-the-Art and Future Directions for Modeling and Simulation in Engineering Dynamics Applications. *ASCE-ASME J Risk and Uncert in Engrg Sys Part B Mech Engrg*, 6(3), 05 2020. ISSN 2332-9017. doi: 10.1115/1.4046739. URL https://doi.org/10.1115/1.4046739. 030901.

[8] Adam Mentsiev and Islam Mutaev. Automation and control of thermal processes in the furnace. *IOP Conference Series: Materials Science and Engineering*, 734:012212, 01 2020. doi: 10.1088/1757-899X/734/1/012212.

[9] Bin Xu, June Wang, Xinping Wang, Zhihong Liang, Liming Cui, Xiao Liu, and Anthony Ku. A Case Study of Digital-Twin-Modelling Analysis on Power-Plant-Performance Optimizations. *Clean Energy*, 3:227–234, 11 2019. doi: 10.1093/ce/zkz025.

[10] Stephen E Zitney. Dynamic Model-Based Digital Twin, Optimization, and Control Technologies for Improving Flexible Power Plant Operations, 2 2019. URL https://www.osti.gov/biblio/1502381.

[11] Vijaya Damodara, Arokiaraj Alphones, Daniel Chen, Helen Lou, Christopher Martin, and Xianchang Li. Flare performance modeling and set point determination using artificial neural networks. *International Journal of Energy and Environmental Engineering*, 11, 08 2019. doi: 10.1007/s40095-019-00314-3.

[12] Jennifer P. Spinti, Philip J. Smith, and Sean T. Smith. Atikokan digital twin: Machine learning in a biomass energy system. *Applied Energy*, 310:118436, 2022. ISSN 0306-2619. doi: https://doi.org/10.1016/j.apenergy.2021.118436. URL https://www.sciencedirect.com/science/article/pii/S0306261921016627.

[13] James O Berger. *Statistical decision theory and Bayesian analysis; 2nd ed.* Springer series in statistics. Springer, New York, 1985. doi: 10.1007/978-1-4757-4286-2. URL https://cds.cern.ch/record/1327974.

[14] Marc McDaniel. Flare Efficiency Study. Technical Report Report No. 600/2-83-052, United States Environmental Protection Agency: Washington DC, 1983.

[15] United States Government : Code of Federal Regulations, January 2022. URL https://www.ecfr.gov/current/title-40/chapter-I/subchapter-C. National Emission Standards for Hazardous Air Pollutants from Petroleum Refineries: Requirements for Flare Control Devices.

[16] U.S. EPA Office of Air Quality Planning and Standards (OAQPS). Parameters for Properly Designed and Operated Flares. Technical report, Flare Review Panel, April 2012. URL https://www3.epa.gov/airtoxics/flare/2012flaretechreport.pdf. Accessed: 2022-01-01.